Refined Numerical Solution of the Transonic Flow Past a Wedge

S-M. Liang* and K-Y. Fung†
University of Arizona, Tucson, Arizona

A numerical procedure combining the ideas of solving a modified difference equation and of adaptive mesh refinement is introduced. The numerical solution on a fixed grid is improved by using better approximations of the truncation error computed from local subdomain grid refinements. This technique is used to obtain refined solutions of steady, inviscid, transonic flow past a wedge. The effects of truncation error on the pressure distribution, wave drag, sonic line, and shock position are investigated. By comparing the pressure drag to the shocks, a supersonic-to-supersonic shock originating from the wedge shoulder is confirmed.

Introduction

THE problem of interest is flow at subsonic freestream Mach number M_∞ past a wedge (see Fig. 1). After a compression at the leading edge, the flow expands and reaches the sonic condition at the shoulder. Downstream of the shoulder, the flow must return to the subsonic freestream condition through a shock, or shocks. Because of its simplicity, this model was used by Cole[1] and Yoshihara[2] to study the characteristics of transonic flow and the validity of the transonic small-disturbance equation. However, because of the inherent limitations of the hodograph method used in their studies, certain assumptions regarding the flow pattern were made in order to have a complete specification of the problem in the hodograph plane. Cole assumed that the sonic line is locally vertical and contended that the Prandtl-Meyer expansion at the wedge shoulder be terminated by an oblique shock, whereas Yoshihara assumed that a smooth overexpansion occurs at the shoulder and the supersonic zone is terminated by a normal shock downstream of the shoulder. The flow was studied experimentally by Liepmann and Bryson,[3] whose results were inconclusive about the oblique shock at the shoulder due to viscous effects, and numerically by Yu and Seebass,[4] whose solution was inaccurate due to the numerical scheme used and insufficient resolution at the shoulder. To date, no accurate solution describing the correct flow structure has been reported.

Realizing that the flow structure is a result of the expansion at the shoulder where small variations in flow variables may affect the overall flow structure, we apply a subgrid refinement procedure (suggested by Fung et al.[5]), which allows local, as well as global, improvement to obtain a refined solution on a fixed grid without changing the base grid structure, as is needed in other grid refinement procedures. In this procedure, a solution is defined on a fixed grid and is improved through approximation of the truncation error, which is usually ignored in a conventional finite-difference approximation. It is demonstrated in this study that local refinement yields results as accurate as those obtained on a uniformly refined grid, that the truncation error is an effective means for measuring error in the solution of a difference equation and for improving a numerical solution on a fixed grid, and that the procedure suggested by Fung et al.[5] achieves substantial savings in computer time and storage with minimal bookkeeping effort.

A sequence of improved solutions obtained using this method indicates the existence of both an oblique shock near the shoulder and a normal shock downstream of it.

Presented as Paper 85-1593 at the AIAA 18th Fluid Dynamics, Plasmadynamics and Lasers Conference, Cincinnati, OH, July 16-18, 1985; received March 6, 1986; revision received July 24, 1986.

*Ph.D. Candidate, Program in Applied Mathematics, Department of Mathematics; presently, Associate Professor, National Cheng-Kung University, Taiwan.

†Associate Professor, Aerospace and Mechanical Engineering. Member AIAA.

Governing Equation and Numerical Scheme

The governing equation for this flow is the transonic, small-disturbance potential equation:

$$[K\phi_x - (\phi_x^2/2)]_x + \phi_{yy} = 0 \tag{1}$$

Here, the perturbed velocity potential ϕ and the space coordinates x and y have been scaled properly. K, the transonic similarity parameter, is a result of the scaling, which involves the freestream Mach number, the wedge half thickness θ, and the ratio of specific heats γ. The boundary condition on the body is the tangency condition,

$$\phi_y(x,0) = 0, \qquad x > 1$$
$$= 1, \qquad 0 \le x \le 1$$

and the far-field boundary conditions are

$$\phi_x = \phi_y = 0 \text{ as } x^2 + y^2 \to \infty$$

For computational efficiency, this condition may be replaced by an analytical expression for ϕ corresponding to a source singularity at point (½, 0).

Equation (1) admits weak solutions that satisfy the shock jump condition

$$(K - \tilde{\phi}_x)[\phi_x]^2 + [\phi_y]^2 = 0 \tag{2}$$

where the tilde denotes an average quantity across the shock and the brackets denote the jump in the argument.

A balance of x momentum requires that the pressure drag on the wedge be related to the shock jumps, i.e.,

$$\int_{\text{body}} C_p \phi_y(x,0)\mathrm{d}x = -\int_0^1 2\phi_x \mathrm{d}x = -\frac{1}{6}\int_{\text{shocks}} [\phi_x]^3 \mathrm{d}y \tag{3}$$

This equation is used later for evaluating the accuracy of the results.

Equation (1) is discretized using the monotone scheme suggested by Engquist and Osher,[6] and the resultant difference equations are solved by a line relaxation method.

Truncation Error and Grid Refinement

The difference between a differential equation $\mathcal{L}\phi=0$ and the difference equation that models it is the truncation error (denoted as TE hereafter), i.e.,

$$\mathcal{L}\phi = L_h\phi + \mathrm{TE}(\phi,h)$$

Here, $\mathcal{L}$ is the differential operator; ϕ, the solution; and L_h, the difference operator resulting from retention of appropriate leading terms in a Taylor's series expansion on a grid of typical spacing h.

Ordinarily, the discrete system, $L_h\tilde{\phi}_h=0$, is solved for an approximate $\tilde{\phi}_h$ and the TE is assumed to be small. Unfortunately, unless the local grid size is comparable to, or smaller than, the local length scale of the solution, the local TE will be large, causing an error in $\tilde{\phi}_h$. Attempts and limited successes have been reported on various adaptive grid distribution procedures (e.g., Pearson[7] and Babuska[8]), which tend to minimize the local TE. However, these methods very often depend on the criteria used and are sensitive to the control parameters introduced in the procedure for relating the grid sizes to the measures of error. In Ref. 5, Fung et al. explained that it should be possible to obtain at the node points of a grid the values of the exact solution to a differential equation if the TE were known. This means that if the goal is to improve the numerical solution, the basic grid structure does not have to be changed—only improved values of the TE need to be provided.

It can be shown that if the exact solution ϕ were known, the TE can be computed exactly by applying the operator L_h to ϕ, e.g.,

$$\mathrm{TE}(\phi,h) = -L_h\phi$$

Hence, if $\phi_{h/N}$ is the refined solution on the grid of size h/N (i.e., subdividing the base grid of size h, N times), the operation

$$-L_h\phi_{h/N} \equiv \mathrm{TE}_{h/N} \simeq \mathrm{TE}(\phi,h)$$

would yield better approximations of the TE as the refinement factor N increases. Of course, this is true only if the scheme is consistent with the differential equation being approximated; i.e., the truncation error on the finest subgrid diminishes while the truncation error on the base grid approaches the asymptote.

To effect an improved solution on a fixed grid by TE inclusion, we use the procedure suggested by Fung et al.[5] To begin, we choose a base grid, which will not change throughout the procedure. The TE is set to zero, and the discrete equation

$$L_h\phi_h + \mathrm{TE} = 0 \tag{4}$$

is solved for the first approximation ϕ_h^0. Regarding ϕ_h^0 as a refined solution for a grid of size $2h$, an estimate of the TE is then formed by computing

$$L_{2h}\phi_h^0$$

The regions where the estimated TE, $-L_{2h}\phi_h^0$, is larger than a preset value τ are identified; if the base grid was properly chosen, these regions should be a small part of the base region. With boundary conditions interpolated from the base solution, refined solutions satisfying

$$L_{h/N}\phi_{h/N} = 0$$

are then obained and used to form the approximated TE, $-L_h\phi_{h/N}$. Outside the region where refinement is needed, the TE is assumed to remain zero. The process is repeated with the newly obtained $\mathrm{TE}_{h/N}$ until

$$|L_h\phi_{h/M}^{k+1} - L_h\phi_{h/N}^{k}| < \delta \quad \text{for all } M > N$$

This procedure is shown schematically in Fig. 2.

It was shown by Fung et al.[5] how, for various cases, this procedure can lead to improvement of numerical solution on a fixed grid, including the sharpness of shocks. A similar procedure has been suggested by Brandt.[9] He pointed out that nesting subgrids can be coupled with the multigrid procedure, which has been widely used for accelerating the convergence of numerical schemes.

Results and Discussion

The base grid for all of the numerical results is a uniform grid of spacing $h=0.1$ over a computational domain of size 6×6 wedge chords. Figure 3 shows the distribution of the estimated TE, $L_{2h}\phi_h^0$, computed after obtaining the initial base solution ϕ_h^0. The values shown have been multiplied by a factor of 10. Subregions outside of which the maximum TE is less than the preset τ are shown in Fig. 4. No attempts were made to tailor these regions to the minimal sizes. The case of $\tau=0$ means that the whole domain is refined. For the case of $\tau=3.0$, two regions were identified; one is about the leading edge and the other about the shoulder, as expected. Local solutions over these regions were then obtained with interpolated boundary conditions from ϕ_h^0 (for details, see Ref. 10). From the local refined solution, the approximated truncation error is then computed and used to obtain the next refined solution, ϕ_h^1, on the base grid satisfying Eq. (4).

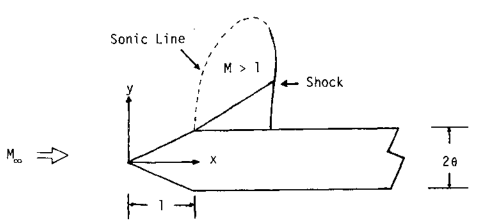

Fig. 1 Flow over a wedge at a transonic Mach number.

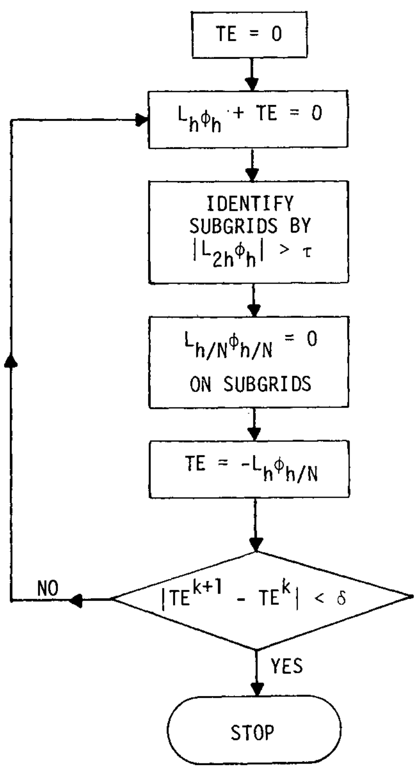

Fig. 2 Schematic of adaptive grid refinement with truncation error injection.

Table 1 Comparison of drag values for different values of τ after the first refinement cycle

Refinement cycle, k	Preset tolerance, τ	Pressure drag	Wave drag due to shocks Oblique	Normal	Total	CPU on CRAY X-MP, s	Relative error of wave drag, %
0	—	0.750	0.300	0.538	0.838	33	12
1	0.00	0.772	0.201	0.610	0.811	629	5
1	0.05	0.773	0.202	0.608	0.810	66	5
1	0.50	0.770	0.179	0.627	0.806	53	5
1	3.00	0.784	0.244	0.575	0.819	50	5

Table 2 Comparison of the drag values after different cycles of refinement, $\tau = 0.05$

Refinement cycle, k	Grid refinement factor, N	Pressure drag	Wave drag due to shocks Oblique	Normal	Total	CPU on CRAY X-MP, s	Relative error of wave drag, %
0	1	0.750	0.300	0.538	0.838	33	12
1	2	0.773	0.202	0.608	0.810	66	5
2	2	0.773	0.202	0.608	0.810	78	5
2	4	0.793	0.129	0.672	0.801	255	1

Fig. 3 Distribution of the estimated truncation error, $L_{2h}\phi_h$ (values have been multiplied by 10).

0.	0.	0.	0.	0.	0.	0.	0.	0.	0.	0.	0.	0.	0.	0.	0.	0.	0.	0.	0.	0.
0.	0.	0.	0.	0.	0.	0.	0.	0.	0.	0.	0.	0.	0.	0.	0.	0.	0.	0.	0.	0.
0.	0.	0.	0.	0.	0.	0.	0.	0.	0.	0.	0.	0.	0.	0.	0.	0.	1.	0.	0.	0.
0.	0.	0.	0.	0.	0.	0.	0.	0.	0.	0.	0.	0.	0.	0.	0.	0.	0.	0.	0.	0.
0.	0.	0.	0.	0.	0.	0.	0.	0.	0.	0.	0.	0.	0.	0.	0.	1.	-2.	0.	0.	0.
0.	0.	0.	0.	0.	0.	0.	0.	0.	0.	0.	0.	0.	0.	0.	1.	1.	-3.	0.	0.	0.
0.	0.	0.	0.	0.	0.	0.	0.	0.	0.	0.	0.	0.	0.	0.	1.	1.	-1.	0.	0.	0.
0.	0.	0.	0.	0.	0.	0.	0.	0.	0.	0.	0.	0.	0.	1.	2.	1.	-1.	-3.	0.	0.
0.	0.	0.	0.	0.	0.	0.	0.	0.	0.	0.	0.	0.	0.	2.	2.	1.	-1.	-5.	1.	0.
0.	0.	0.	0.	0.	0.	0.	0.	0.	0.	0.	0.	0.	2.	3.	1.	-1.	-3.	-3.	1.	0.
0.	0.	0.	0.	0.	0.	0.	0.	0.	0.	0.	0.	1.	4.	3.	0.	-4.	-5.	2.	0.	0.
0.	0.	0.	0.	0.	0.	0.	0.	0.	0.	0.	0.	4.	5.	1.	-5.	-6.	-4.	6.	0.	0.
0.	0.	0.	0.	0.	0.	0.	0.	0.	0.	-1.	1.	9.	3.	-6.	-8.	-4.	-3.	8.	0.	0.
0.	0.	0.	1.	1.	-1.	-1.	0.	0.	0.	-6.	13.	9.	-10.	-13.	-3.	1.	-5.	9.	0.	0.
0.	0.	0.	1.	6.	-10.	-3.	0.	0.	1.	-7.	37.	-26.	-21.	0.	2.	1.	-7.	11.	0.	0.
0.	0.	-1.	-5.	-44.	-55.	15.	2.	1.	1.	-6.	-98.	10.	11.	2.	1.	1.	-8.	11.	0.	0.

↑ LEADING EDGE ↑ SHOULDER

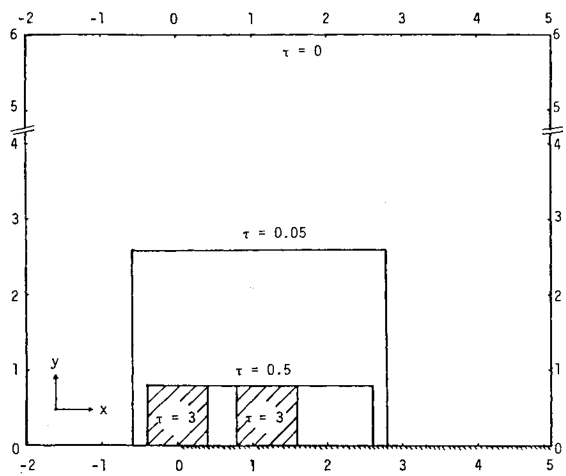

Fig. 4 Computational domain and subregions for various grid refinements.

Figure 5 compares the base solutions before and after the first cycle of refinement with that obtained on a uniformly refined grid size of $h/2$. It shows that this refinement procedure is accurate and efficient. The effects of the refinement with TE injection on the sonic line and on the shock are shown in Fig. 6. Because of the improvement at the shoulder, the normal shock moves downstream and becomes stronger. Table 1 compares values of the pressure drag on the shoulder and the wave drag due to the shocks [according to Eq. (3)] obtained for different values of τ which correspond to different regions of refinement. It is quite clear from this comparison that a subregion of $\tau = 0.05$ is adequate for accurate calculations. The difference between the wave and the pressure drag diminishes after one cycle of refinement from 12 to 5%, at a cost of only twice the computation time needed for the base solution. This is a substantial savings relative to a uniformly refined solution, which costs 20 times as much as the base grid solution ϕ_h^0. It is shown that further savings in computation time are possible with minor losses in accuracy. Another cycle of refinement, keeping the refinement factor the same ($N=2$) but using boundary conditions from the base solution for the local refined solution, showed that the effects due to the newly updated boundary conditions on the base solution were minor compared to those of increasing N. The difference in the drag values is reduced to less than 1% after two cycles of refinement, $k=2$, and for a refinement factor $N=4$, but to only 5% if $N=2$ (Table 2). For two cycles with $N=4$, the computation time was 255 s, approximately four times that for one cycle because the total number of grid points was increased by the same factor; a better strategy would be to apply the adaptive refinement procedure to the local solution coupled with a pattern recognition routine to determine the subgrid geometry, as demonstrated by Berger and Oliger,[11] instead of the uniform refinement. The base solution obtained after two cycles of refinement was accurate within 1% in the drag values, the same order of magnitude as the maximum residual of the difference equation. Further refinements are not needed unless the residual tolerance is set to a smaller value in solving the difference equations.

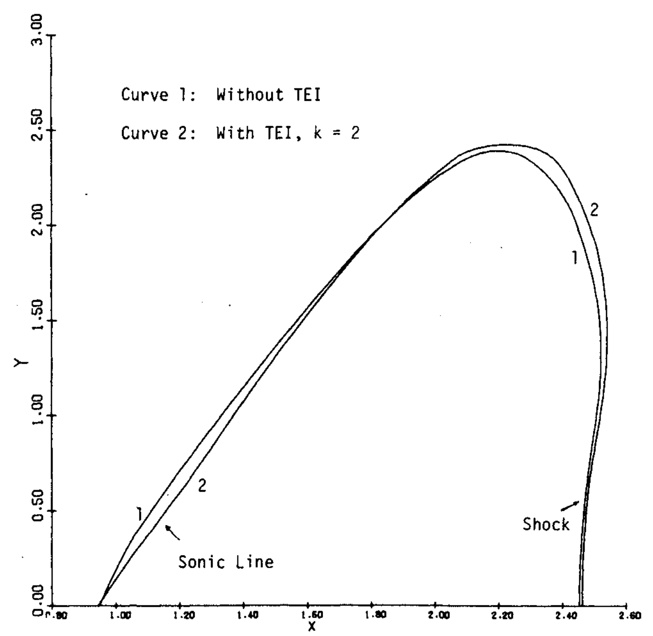

Fig. 5 Comparison of results after the first cycle of refinement, $K=0.5$.

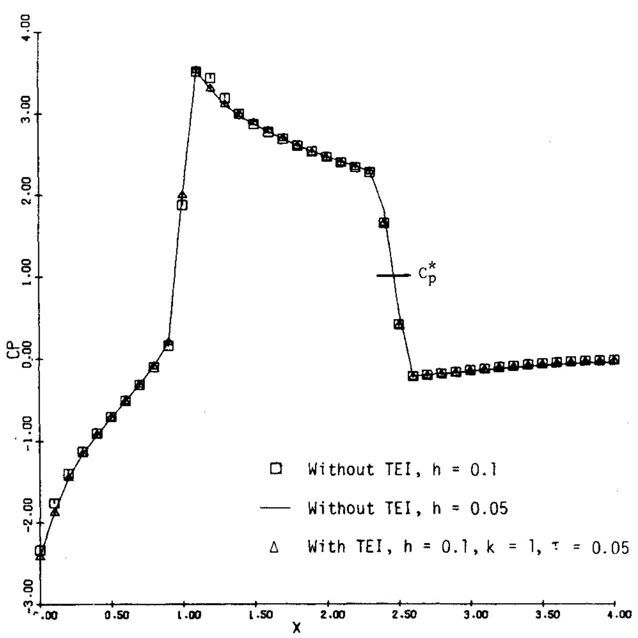

Fig. 6 Effects of truncation error injection on the sonic line and shock location, $K=0.5$.

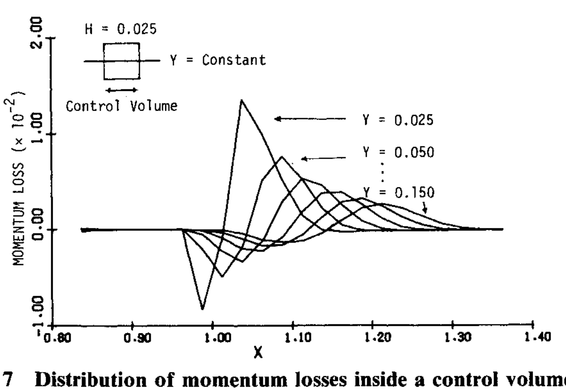

Fig. 7 Distribution of momentum losses inside a control volume at different values of y, $K=0.5$.

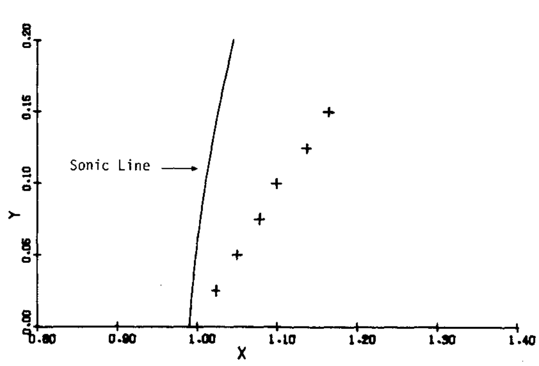

Fig. 8 Sonic line and oblique shock, $K=0.5$.

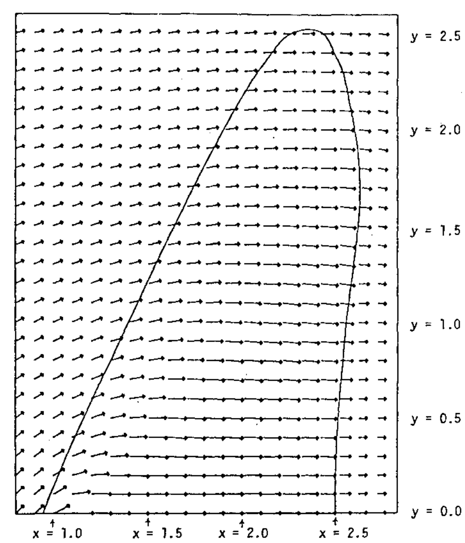

Fig. 9 Velocity field at the sonic bubble, $K=0.5$.

In evaluating the shock drag, one notices that the drag due to the normal shock is about four-fifths of the pressure drag on the shoulder. To detect the momentum loss, we moved a control volume along a grid line parallel to the x axis and computed the losses at different x stations. These values are plotted in Fig. 7. The coordinates of the midpoint between a maximum and a minimum are shown by the crosses in Fig. 8, indicating the location of an oblique shock at an angle of about 41 deg with the x axis due to the compression immediately after the Prandtl-Meyer expansion.

A close look at the velocity field in Fig. 9 reveals the qualitative structure of the flow at the shoulder, which is of prime interest. By measuring the flow angle, it is found that the flow overexpands as much as -3.1 deg at a point 0.3 chord above and 0.6 chord downstream from the shoulder. A local analysis[12] shows that the flow expands to a maximum velocity

$$u(1^+,0)=K+(3/2)^{2/3}=1.810$$

right after the shoulder and compresses along the wall at the rate

$$u=(3/2)^{2/3}(1-2^{-8/3}3x^{2/3})+K$$

which is quite close to the numerical prediction. Because of the compression, the characteristics coalesce into a weak shock wave starting with a slope of $(2/3)^{1/3}\simeq 41$ deg, a zero curvature, and a negative third derivative. The maximum velocity, linearly extrapolated from downstream to the shoulder, assumes the value 1.878 on the base grid and the values 1.864 and 1.819 after the first and second cycles of refinement, respectively, approaching the theoretical value as the solution on the base grid is improved. It is this oblique shock that accounts for the balance of momentum.

Conclusions

An efficient refinement procedure combining the ideas of solving a modified difference equation and of adaptive mesh refinement has been developed for refined computations of steady, inviscid, transonic flows. The advantage of this procedure is that it allows local, as well as global, improvement on a base solution without changing the base grid structure and with only modest increases in storage and computation time.

In the computation of the flow over a wedge at $K=0.5$, the existence of an oblique shock near the shoulder is confirmed by comparing the pressure drag and the wave drag.

Although the present method is applied to obtain solutions of the small-disturbance equation for a particular profile, it can be extended, in principle, to other complicated flow problems.

Acknowledgments

This research was carried out in the Computational Fluid Mechanics Laboratory of the Aerospace and Mechanical Engineering Department under AFOSR Grant 83-0071, monitored by Dr. James D. Wilson, and NASA CFD Traineeship Grant NGT 03-002-800. Permission from Dr. Paul Kutler to use the NASA Ames CRAY X-MP computer for this and other studies related to the trainseeship program is gratefully acknowledged.

References

[1]Cole, J. D., "Drag of a Finite Wedge at High Subsonic Speed," *Journal of Mathematics and Physics*, Vol. 30, 1951, pp. 79–93.

[2]Yoshihara, H., "On the Flow Over a Finite Wedge in the Lower Transonic Region," WADC Tech, Rept. 56-444, ASTIA Doc. AD 110428, June 1956.

[3]Liepmann, H. W. and Bryson, A. E. Jr., "Transonic Flow Past Wedge Sections," *Journal of the Aeronautical Sciences*, Vol. 17, 1950, pp. 745–755.

[4]Yu, N. J. and Seebass, A. R., "Inviscid Transonic Flow Computations with Shock Fitting," *Symposium Transsonicum II*, edited by K. Oswatitsch and D. Rues, Springer-Verlag, New York, 1976, pp. 449–456.

[5]Fung, K-Y., Tripp, J., and Goble, B., "Adaptive Refinement with Truncation Error Injection," University of Arizona EES Rept. CRML 84-01, 1984, to appear in *Computer Methods in Applied Mechanics and Engineering*.

[6]Engquist, B. and Osher, S., "Stable and Entropy Satisfying Approximations for Transonic Flow Calculations," *Mathematics of Computation*, Vol. 34, 1980, pp. 45–75.

[7]Pearson, C. E., "On a Differential Equation of Boundary Layer Type," *Journal of Mathematics and Physics*, Vol. 47, 1968, pp. 134–154.

[8]Babuska, I., "The Self-Adaptive Approach in the Finite Element Method," *The Mathematics of Finite Elements and Applications*, Vol. 11, MAFELAP, 1975, edited by J. R. Whiteman, Academic, 1976.

[9]Brandt, A., "Multi-Level Adaptive Solutions to Boundary Value Problems," *Mathematics of Computation*, Vol. 31, 1977, pp. 333–390.

[10]Liang, S-M., "Refined Numerical Solutions of the Transonic Flow Past a Wedge," Ph.D. dissertation, Univ. of Arizona, 1984.

[11]Berger, M. J. and Oliger, J., "Adaptive Mesh Refinement for Hyperbolic Partial Differential Equations," *Journal of Computational Physics*, Vol. 53, 1984, pp. 484–512.

[12]Sobieczky, H., "Transonic Wedge Shoulder Flow Singularity," Univ. of Arizona Rept. CFML 85-04, 1985.